Title

Interfacial charge transfer in Pt-loaded TiO2 P25 photocatalysts studied by in-situ diffuse reflectance FTIR spectroscopy of adsorbed CO

Authors

Litke, Anton
Frei, Heinz
Hensen, Emiel JM
et al.

Publication Date

2019-02-01

DOI

10.1016/j.jphotochem.2018.10.023

Peer reviewed

Influence of above-bandgap excitation on Pt-loaded TiO_2 and CdS photocatalysts studied by FTIR spectroscopy of adsorbed CO

Anton Litke, Heinz M. Frei, Emiel J.M. Hensen,* Jan P. Hofmann*

Corresponding authors:

* J.P. Hofmann e-mail: J.P.Hofmann@tue.nl; phone: +31 (0) 40 247 3466

* E.J.M. Hensen e-mail: E.J.M.Hensen@tue.nl; phone: +31 (0) 40 247 5178

Abstract

Loading of inorganic semiconductors with metal co-catalysts is commonly used to improve the activity of photocatalytic systems, which depends on charge carrier trapping and utilization by co-catalyst particles. The electrochemical potential at the interface between an electrolyte and a metal-loaded semiconducting photocatalyst can be monitored *in-situ* via the shift of the vibrational frequency of adsorbed CO. Here, we explored a similar approach to probe the gas/solid interface of photoplatinized TiO_2 and CdS photocatalysts. Contrary to a recent report, we did not observe prominent shifts of the adsorbed CO bands which can be unambiguously attributed to charging of the Pt cocatalyst nanoparticles. The most prominent blue shift of *ca.* 0.5 cm^{-1} was observed for the 2114-2112 cm^{-1} band of CO adsorbed on atomic Pt species. However, heating of the system to 383 K resulted in a similar band shift. This demonstrates that the difference in dielectric properties between aqueous electrolytes and vacuum are critical for the development of prominent shifts of adsorbed CO bands upon trapping of photogenerated charge carriers on co-catalyst particles. Prolonged exposure of Pt-TiO_2 without pre-adsorbed CO to 325 nm irradiation led to the formation of bands at 2114 cm^{-1} and 2056 cm^{-1}, which evidenced photocatalytic formation of CO and hydrogen from water and adventitious organic compounds adsorbed on Pt-TiO_2. This demonstrates the importance of well-defined sample pretreatment procedures and control over contaminants.. The experimental findings are discussed in terms of an electrostatic Stark

effect, charge screening, co-adsorption, coverage-dependent shifts of the vibrational bands of adsorbed CO and photocatalytic surface reactions.

INTRODUCTION

Solar-driven chemical energy conversion, production of chemicals and remediation of pollutants have attracted substantial research efforts over the last decades.[1–3] Sunlight is the most abundant renewable energy source on Earth. The main challenge of the transition toward a solar-powered economy is the intermittency of solar light which requires a scalable technology to convert, store and transport solar energy in a convenient form. In this regard, production of solar fuels (*e.g.* H_2, CH_4, alcohols) by means of photocatalytic water splitting and CO_2 reduction can be promising solutions.[3–8] However, most photocatalytic systems have rather low solar-to-chemical energy conversion efficiencies. The performance of a photocatalytic system can be improved by loading suitable co-catalysts which increase selectivity and lower over-potentials of the desired redox reactions.[9,10] Also, co-catalysts aid separation and utilization of photogenerated charge carriers which determine the activity of a photocatalytic material. Consequently, a detailed understanding of these processes is of utmost importance for the optimal design of such systems.

Light-induced processes in inorganic semiconductor photocatalysts can be studied by mid-infrared spectroscopy. This technique can access both the molecular species present at the semiconductor interface and the dynamics of majority charge carriers.[11–16] Small probe molecules such as CO are sensitive to the electronic structure of adsorption sites[17] and, therefore, are

widely used to probe Lewis and Brønsted acid sites in solid catalysts and to study the oxidation state and distribution of supported metal nanoparticles by means of vibrational spectroscopies.[19] Moreover, light-induced changes of the electrochemical potential at the semiconductor/liquid interface can be monitored *in-situ* via the shifts of vibrational bands of CO adsorbed on metal co-catalyst particles.[20,21] Although being informative, experiments with liquid/solid systems require specialized accessories for attenuated total reflection or external reflection as well as accurate correction for the solvent absorption which complicates data collection and processing.[16] On the other hand, Shen et al. recently reported an 11 cm^{-1} red shift of the vibrational band of CO adsorbed at the gas/solid interface, when platinized TiO_2 was exposed to UV irradiation.[22] The observed shift was ascribed to the transfer of photogenerated electrons from titania to the Pt nanoparticles. This effect can be used to understand how loading, dispersion, and oxidation state of the metal co-catalyst affect charge carrier transfer and utilization in co-catalyst loaded photocatalytic systems.

To the best of our knowledge, the work of Shen et al.[22] is the only study reporting such prominent light-induced shifts of the adsorbed CO band for gas/solid systems. In the present work, we systematically studied this effect for platinized TiO_2- and CdS-based photocatalysts by steady-stated and time-resolved diffuse reflection FTIR spectroscopy (DRIFTS) under well-defined conditions. Contrary to literature, we did not observe any prominent shifts of the vibrational bands of CO adsorbed on platinized photocatalysts at the

time scale ranging from sub-seconds to minutes. The largest light-induced blue shift of *ca.* 0.5 cm^{-1} was observed for the 2112-2114 cm^{-1} band of CO adsorbed on isolated Pt atoms present in Pt-TiO_2 sample. A similar band rearrangement was observed when this sample was heated to 383 K in the dark. Apart from this, we found that prolonged UV irradiation of Pt-TiO_2 (> 10 min) led to the *in-situ* formation of CO and development of IR bands at 2115 cm^{-1} and 2057 cm^{-1}. The development of these bands was substantially slower in an oxidized sample as compared to the untreated material. Oxidized Pt-TiO_2 also exhibited a lower content of organic adsorbates, demonstrating the importance of sample pre-treatment. In summary, our results show that the above-bandgap excitation of Pt-loaded inorganic semiconductors does not induce any prominent shifts of the IR bands of CO adsorbed at the gas/solid interface which can be unambiguously attributed to charging of the co-catalyst particles. This can be due to inefficient charge carrier transfer under the applied experimental conditions, screening of the transferred charges by the d-band of the Pt nanoparticles or the low dielectric permittivity of the medium. These outcomes are discussed in terms of the electrostatic Stark effect, surface photovoltage, screening of the transferred charge by the metal d-band and coverage-dependent vibrational frequencies of CO adsorbed on Pt.

EXPERIMENTAL DETAILS

Chemicals. Aeroxide P25 TiO_2 (Evonik Industries), NaOH (Sigma Aldrich, ≥98%), $Cd(CH_3COO)_2 \cdot 2H_2O$ (Sigma Aldrich, ≥98%), $Na_2S \cdot 9H_2O$ (Sigma Aldrich, ≥98%), Na_2SO_3 (Sigma Aldrich, 98 – 100%), $H_2PtCl_6 \cdot nH_2O$ (Sigma-Aldrich, ≥ 38% Pt basis), D_2O (Cambridge Isotope Laboratories, 99.90% D), methanol (VWR, technical grade) and ethanol absolute (VWR, technical grade) were used as received without further purification. Demineralized water (>15 MΩ·cm at 298 K) was used for preparation of solutions, synthesis and washing of the samples. CO (the Linde Group, ≥99.99%) and D_2 (Sigma-Aldrich, 99.96 at.%) were used as delivered without further purification. O_2 (≥ 99.95%), H_2 (≥ 99.999%) and He (≥ 99.999%) supplied by the Linde Group were passed through moisture and/or oxygen filters (Agilent technologies).

Pt-CdS synthesis. CdS was prepared from the corresponding insoluble hydroxide using a hydrothermal method described in literature.[23] Briefly, the insoluble hydroxide was precipitated by adding 15 mL aqueous NaOH (8.2×10^{-3} mol) to 30 mL aqueous $Cd(NO_3)_2 \cdot 4H_2O$ (4.1×10^{-3} mol). The white dispersion was stirred for 15 min and the solid product was separated by centrifugation, washed three times with demineralized water and re-dispersed in 35 mL 1.0 M CH_3COONa in a PTFE-lined stainless steel autoclave (45 mL capacity). Then, 4.51×10^{-3} mol thioacetamide (10% sulphur excess) was added to this dispersion under stirring. The autoclave was sealed, placed in an oven at 180 ˚C and kept under continuous tumbling for 24 h. After this, the autoclave was cooled down to room temperature and the yellow-orange

solid product was collected by centrifugation, washed three times with demineralized water and dried under vacuum at room temperature.

The resulting CdS was loaded with 0.5 wt.% Pt according to the modified procedure described in literature.[24] To this end, 100 mg CdS was dispersed in 50 mL 1.0 M NaOH containing H_2PtCl_6 in the amount equivalent to 0.5 mg Pt and transferred into a side-illuminated PEEK cell equipped with a quartz optical window. The dispersion was degassed under vacuum and illuminated under continuous stirring for 3 h. The 500 W Hg(Xe) lamp equipped with an IR water filter and a 420 nm UV cut-off glass filter (OD^{410} = 5.0) was used as light source. The solid product was separated by centrifugation, washed three times with demineralized water and dried under vacuum at room temperature. This sample is denoted Pt-CdS.

Pt-TiO_2 synthesis. 0.5 wt.% Pt was photodeposited on commercial Aeroxide P25. Briefly, 500 mg TiO_2 were dispersed under continuous stirring in 90 mL 10 vol.% aqueous CH_3OH containing 2.5 mg Pt in the form of H_2PtCl_6. The dispersion was transferred in a double-walled glass reactor with a top-mounted quartz window, degassed and irradiated with the full spectrum of the 500 W Hg(Xe) lamp (Newport, USA). The lamp was equipped with an IR water filter and a full spectrum turning mirror. The suspension was irradiated for 1 h and a grey-brownish solid was separated by centrifugation, washed twice with demineralized water and dried under vacuum at room temperature.

Oxidative treatment of Pt-TiO_2. In order to remove organic adsorbates present on Pt-TiO_2 the sample was pre-treated as follows. The material was placed in an *in-situ* low-temperature chamber (Harrick Scientific), evacuated to the lowest stable pressure (*ca.* < 10^{-3} mbar) and kept under dynamic vacuum for 0.5 h. Then we added 100 mbar O_2, heated the sample to 523 K and irradiated with the 325 nm line of continuous-wave He-Cd laser (Kimmon Koha). The light intensity at the optical window of the DRIFTS cell was *ca.* 10 mW/cm^2. This treatment removed a substantial amount of hydrocarbons and oxygenates present on the untreated material

Characterization. Morphology of the samples and Pt particle size distribution were studied by bright field transmission electron microscopy (FEI Technai G2, 200 kV). Powder XRD patterns were collected on a Bragg-Brentano Bruker Endeavour D2 powder diffractometer equipped with a Cu cathode and a 1D LYNXEYE detector (Ni-filtered K_β, 1.0 mm primary beam slit and 3.0 mm beam knife height). Diffuse-reflectance UV-vis spectra were obtained on a Shimadzu UV-2401PC UV-vis spectrometer equipped with an integrating sphere accessory. $BaSO_4$ was used as a reference for the UV-Vis spectra.

Infrared spectroscopy. All diffuse-reflectance infrared Fourier transform (DRIFT) measurements were carried out on a Bruker Vertex 70v FTIR spectrometer equipped with a liquid-nitrogen cooled MCT detector and a diffuse-reflectance accessory (Praying Mantis, Harrick Scientific). Powder

samples were placed in the low-temperature chamber (Harrick Scientific) equipped with two KBr windows for IR signal collection and one quartz window for UV irradiation of the samples. The spectra were recorded at 4 cm^{-1} resolution in the 3950–600 cm^{-1} range by averaging 100 individual scans. Dry KBr (Sigma Aldrich, IR spectroscopy grade) was used as a reference for the survey DRIFT spectra. The sample in the dark or before exposure to CO was used as the reference for difference spectra. The 325 nm line of a continuous wave Cd-He laser (Kimmon Koha) was used as the light source. Light intensity at the quartz window of the DRIFTS cell was *ca.* 10 mW/cm^2. The exposure time was controlled with an optical shutter (Thorlabs). A low-pass IR filter (cut-off frequency 3950 cm^{-1}) was placed in front of the detector compartment to block stray light and prevent alias back-folding.

RESULTS AND DISCUSSION

The DRIFT spectrum of as-prepared Pt-TiO_2 which was kept under dynamics vacuum ($p < 10^{-3}$ mbar) for 0.5 h in the low-temperature reaction chamber (Harrick Scientific) without any additional treatment is shown in Figure 1, black curve. This spectrum exhibits IR bands of surface hydroxyls of anatase (3725 cm^{-1}, 3632 cm^{-1}) and rutile (3680 cm^{-1}, 3414 cm^{-1}) TiO_2 phases, hydrocarbon moieties (multiple bands in the 3000–2900 cm^{-1} region), molecularly adsorbed water (3400 cm^{-1}, 1624 cm^{-1}), carboxylates or carbonates (1535 cm^{-1}, 1438 cm^{-1}).[25–31]

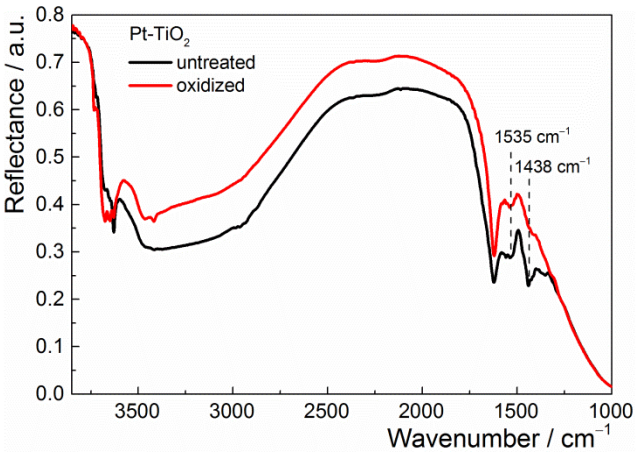

Figure 1. Room temperature DRIFT spectra of untreated and oxidized Pt-TiO_2 in the dark under static vacuum. Note the difference in carboxylic bands intensities (*i.e.* 1535 cm^{-1} and 1438 cm^{-1}) before and after the oxidative treatment.

When untreated Pt-TiO_2 was exposed to 325 nm irradiation under static vacuum (Figure S1, Supporting Information), the bands of molecularly (3400 cm^{-1} and 1624 cm^{-1}) and dissociatively (3695 cm^{-1}, 3632 cm^{-1}) adsorbed water decreased in intensity while those of terminal hydroxyls (3734 cm^{-1} and 3720 cm^{-1}) became more prominent. Besides this, a broad absorption feature emerged in the region below 2000 cm^{-1}. Its intensity increased toward lower wavenumbers and could be fit with an exponential function describing IR absorption due to free conduction band electrons (CBE):[11–14]

$$|.| = A\nu^{-1.7} \qquad (1)$$

where A is the proportionality coefficient and ν is the frequency of IR irradiation in cm^{-1}. After several minutes under UV light, bands at 2115 cm^{-1} and 2057 cm^{-1} emerged in the DRIFT spectrum. Intensities of these bands slowly increased over time under irradiation. In the dark, the 2115 cm^{-1} band was stable for several hours while the 2057 cm^{-1} band lost *ca.* 70% of intensity within the first 10–15 min and then decayed further at slower rates (Figure 2). These bands can be ascribed to CO adsorbed on isolated Pt atoms (2115 cm^{-1}) and metallic Pt particles (2057 cm^{-1}), respectively.[32–35]

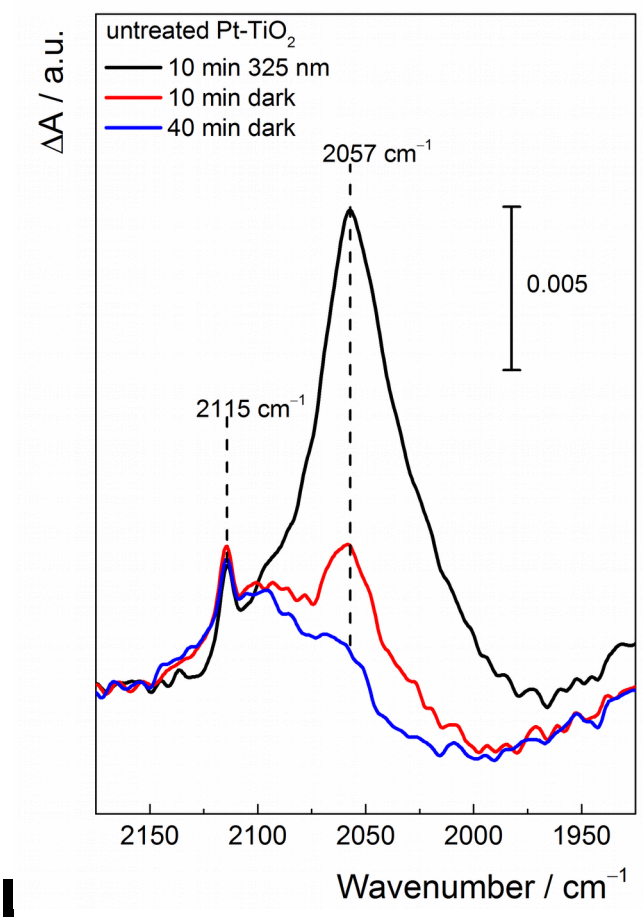

Figure 2. The ν(CO) region of the difference DRIFT spectra of untreated Pt-TiO_2 at 293 K under static vacuum. Sample exposed to 325 nm light for 10

min (black) and the same sample kept in the dark for 10 min (red) and 40 min (blue).

Effect of 325 nm irradiation on CO adsorbed on untreated Pt-TiO_2. When untreated Pt-TiO_2 was exposed to 2.0 mbar CO, bands at 2114 cm^{-1}, 2087 cm^{-1}, 2067 cm^{-1} and 1836 cm^{-1} formed (Figure 3A). The narrow band at 2114 cm^{-1} corresponds to CO adsorbed on isolated Pt atoms.[32] The components at 2087 cm^{-1} and 2063 cm^{-1} were ascribed to CO linearly adsorbed on metallic Pt particles while the band at 1836 cm^{-1} is characteristic for CO adsorbed on Pt metal in bridged configuration.[33–35] Exposure of this sample to 325 nm light induced no apparent shift of the adsorbed CO bands (Figure 3A) even under prolonged irradiation. When the spectra recorded under UV irradiation were referenced to the dark spectrum, minor intensity losses at 2099 cm^{-1}, 2054 cm^{-1} and 1860 cm^{-1} became apparent (Figure 3B, red spectrum). These spectral changes did not relax in the dark completely and some intensity loss at 2114 cm^{-1} was permanent. Repetitive exposure to UV light did not result in accumulation of these effects. Similar spectral changes were observed when Pt-TiO_2 with adsorbed CO was heated from 293 K to 323 K (Figure S2, Supporting Information).

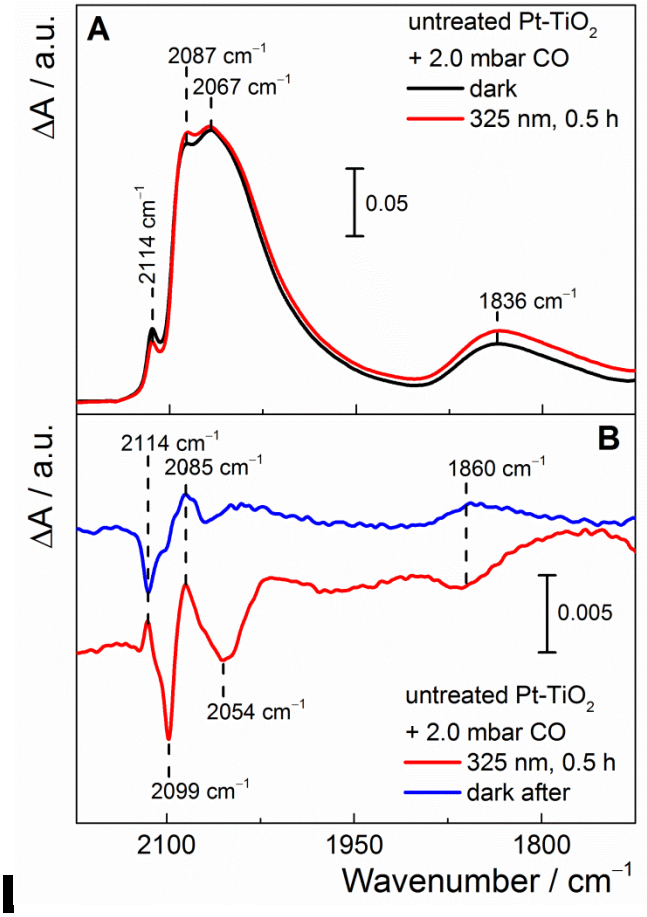

Figure 3 The ν(CO)region of the difference DRIFT spectra of untreated Pt-TiO_2 in contact with 2.0 mbar CO. A – spectra of the sample in the dark (black) and under 325 nm irradiation (red) referenced to the sample before exposure to CO; B – spectra under (red) and after (blue) UV irradiation referenced to the sample before irradiation (black spectrum of A).

Oxidized Pt-TiO_2 under 325 nm irradiation. In order to remove organic adsorbates present on untreated Pt-TiO_2, the material was subjected to an oxidative treatment (*cf.* experimental section). The DRIFT spectrum of the oxidized material is shown in Figure 1, grey curve. Intensities of the CH_x (3000–2900 cm^{-1}) and carboxylates (1535 cm^{-1}, 1438 cm^{-1}) bands became

substantially lower after the treatment.[27,31] When oxidized Pt-TiO_2 was exposed to UV light, the bands of adsorbed water and surface hydroxyls decreased in intensity and the broad CBE absorption feature appeared in the spectrum below 2000 cm^{-1}. Prolonged irradiation of oxidized Pt-TiO_2 led to the formation of bands at 2114 cm^{-1} and 2057 cm^{-1} (Figure S3, Supporting Information). Compared with the untreated sample, these bands developed slower and had lower intensities suggesting that adventitious carbon-containing adsorbates present on TiO_2 were involved in formation of these CO bands.

Effect of 325 nm irradiation on CO adsorbed on oxidized Pt-TiO_2. When oxidized Pt-TiO_2 was exposed to 2.0 mbar CO, several bands appeared in the carbonyl region (Figure 4A). Positions and structure of the bands arising from CO adsorbed on metallic Pt particles in the linear (2087 cm^{-1}, 2067 cm^{-1}) and bridged (1836 cm^{-1}) configuration were similar to those observed in the untreated sample (Figure 3A). This suggests that the oxidative treatment did not cause any prominent sintering, reconstruction or oxidation of the Pt nanoparticles. The main difference between the untreated and oxidized samples was the shift of the 2114 cm^{-1} band to 2112 cm^{-1} after the treatment. No apparent shift of the adsorbed CO bands was observed when oxidized Pt-TiO_2 was exposed to 325 nm irradiation Figure 4B. First exposure of oxidized Pt-TiO_2 to UV light led to a loss of intensity at 2114 cm^{-1} and 2099 cm^{-1} while the components at 2028 cm^{-1} and 1840 cm^{-1} became more prominent. Most of these spectral changes did not recover in the dark

(Figure 4B, blue curve). Repeated exposure to 325 nm irradiation did not lead to any further spectral changes.

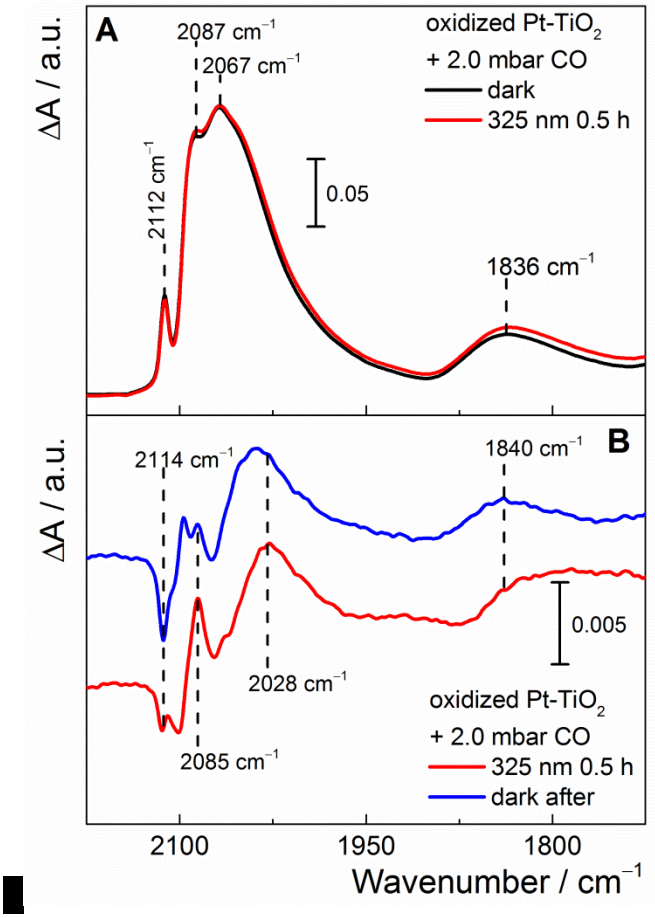

Figure 4 The carbonyl region of the difference DRIFT spectra of oxidized Pt-TiO_2 in contact with 2.0 mbar CO. A – the sample in the dark (black) and under 325 nm irradiation (red) referenced to the sample under vacuum; B – spectra under (red) and after (blue) UV irradiation referenced to the sample before irradiation (black spectrum).

Shift of the 2112 cm^{-1} band (CO adsorbed on atomic Pt species) under 325 nm irradiation. The 2120–2100 cm^{-1} spectral region exhibited

complex band rearrangements, when untreated or oxidized Pt-TiO_2 with adsorbed CO was exposed to 325 nm irradiation (Figures 2B and 4B). Overlapping bands of CO adsorbed on isolated Pt atoms and metal nanoparticles complicated the analysis of these light-induced effects. Hence, we separately studied the effect of UV irradiation on CO adsorbed on isolated Pt atoms. To this end, oxidized Pt-TiO_2 was equilibrated with 2.0 mbar CO for one hour and then evacuated and kept under dynamic vacuum at room temperature for another hour. In this way, CO desorbed from Pt nanoparticles (*i.e.* 2087–2067 cm^{-1} and 1836 cm^{-1} bands almost completely disappeared) and the sample exhibited the well-resolved band at 2112 cm^{-1} with only a minor component at 2084 cm^{-1} (Figure 5). The 2112 cm^{-1} band was stable under dynamic vacuum for hours which agrees with its assignment to CO adsorbed on atomically dispersed Pt.[32]

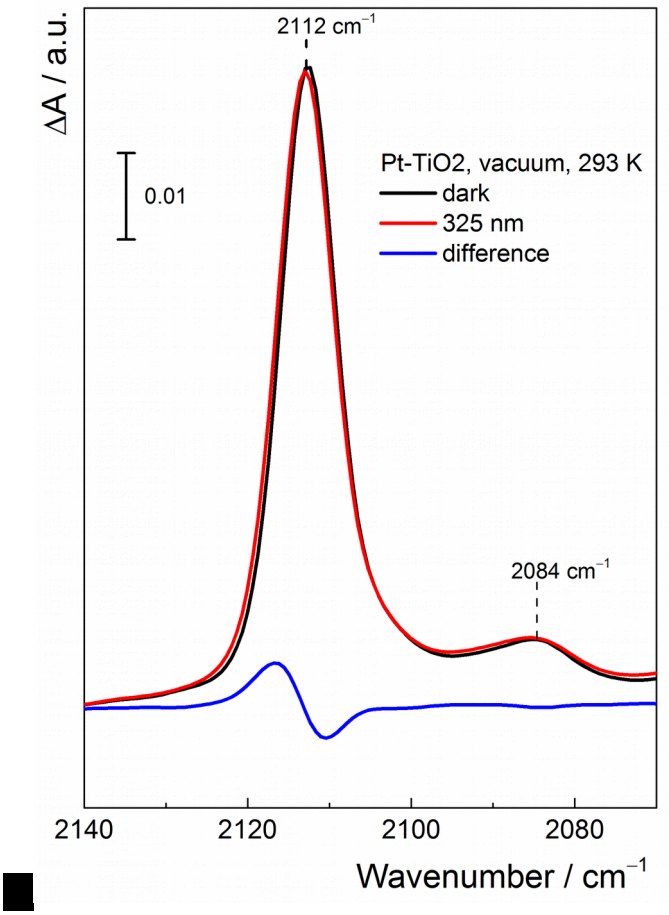

Figure 5. Carbonyl region of the DRIFT spectra of oxidized Pt-TiO_2 under static vacuum at 293 K. The sample in the dark (black), under the 325 nm irradiation (red) and the difference between these two spectra (blue).

When this sample was exposed to 325 nm irradiation, the apparent band maximum shifted from 2112.3 cm^{-1} to 2112.9 cm^{-1} and its full width at half maximum increased from 8.3 cm^{-1} to 8.5 cm^{-1} (Figure 5). These spectral changes reversed in the dark and could originate either from charging of Pt atoms or from the light-induced heating of the material. To test the latter hypothesis, we heated this material under static vacuum in the dark. The 2112 cm^{-1} band experienced a red shift, when the temperature increased

from 273 K to 353 K. However, a blue shift was observed at temperatures above 353 K (Figure S4, Supporting Information). At 383 K, the position and full width at half maximum of the 2112 cm^{-1} carbonyl band were similar to those observed under 325 nm irradiation (*cf.* Figure 5). Hence, the shift of the 2112 cm^{-1} observed under UV irradiation cannot be unambiguously attributed to the interaction of adsorbed CO with photogenerated charge carriers. Moreover, the changes of carbonyl bands induced by the above-bandgap irradiation of Pt-TiO_2 took place at the time scale of minutes while dynamics of photogenerated electron absorption happened at a shorter time scale (Figure S5, Supporting Information). This discrepancy further supports the conclusion that the rearrangements of the adsorbed CO bands observed under above-bandgap irradiation were not caused by the charge carrier transfer between titania and Pt species.

Formation of the 2056 cm^{-1} band upon co-adsorption of CO with hydrogen. Both untreated (Figure 2) and oxidized (Figure S3, Supporting Information) Pt-TiO_2 developed bands at 2114–2112 cm^{-1} and 2056 cm^{-1} under 325 nm irradiation. The 2114–2112 cm^{-1} component originated from CO adsorbed on isolated Pt atoms, while the nature of the 2056 cm^{-1} band was unclear. The 2056 cm^{-1} band was not observed as a separate component when Pt-TiO_2 equilibrated with gaseous CO (Figure 3) neither it appeared upon desorption of CO from the sample under dynamic vacuum (Figure S6, Supporting Information). In the latter case one can expect a red shift of the 2087–2063 cm^{-1} carbonyl bands with decreasing CO coverage due to

weakened dipole coupling among adsorbed CO molecules.[36] Therefore, the 2056 cm^{-1} band cannot be attributed solely to CO adsorbed on Pt nanoparticles at low coverage. On the other hand, the CO band position can be affected by co-adsorption of other species on Pt nanoparticles. For instance, hydrogen can be produced on Pt-TiO_2 upon photocatalytic reduction of adsorbed water at temperatures below 373 K.[37]

In order to evaluate whether *in-situ* formation of hydrogen could result in formation of the ν(CO) band at 2056 cm^{-1}, we exposed oxidized Pt-TiO_2 to molecular H_2. Admission of 1.0 mbar H_2 led to the formation of an asymmetric band with the apparent maximum at 2045 cm^{-1} (Figure 6A). A similar band (2037 cm^{-1}) was observed when a deuterium-exchanged sample was exposed to D_2 gas (Figure 6B). The intensity of these bands did not increase with increasing pressure of H_2 or D_2. This means that they are unlikely due to CO impurities present in the gas feed. On the other hand, they cannot be ascribed to hydride species, because ν(Pt-D) appears in the region around 1470-1420 cm^{-1}.[38,39] When hydrogen was evacuated from the cell, the 2045 cm^{-1} band became narrower and more symmetric. Prolonged evacuation decreased the intensity of this spectral feature while its maximum shifted to 2055 cm^{-1} (Figure 6A). Evacuation of D_2 led to similar spectral changes (Figure 6B). The formation of the band at 2050–2060 cm^{-1} was also observed when the sample with CO adsorbed predominantly on isolated Pt atoms (Figure 5) was exposed to H_2 gas (Figure S8, Supporting Information). The intensity of this band grew at the expense of the 2112 cm^{-1}

component. The latter can be explained by a displacement of CO adsorbed on isolated Pt atoms by hydrogen spilled over from metallic Pt nanoparticles on the oxide.[38] The displaced CO then co-adsorbs with hydrogen on metallic Pt nanoparticles giving rise to the band at 2053-2055 cm^{-1}. Summing up, we conclude that the 2056 cm^{-1} band, which formed under UV irradiation of Pt-TiO_2, corresponds to CO co-adsorbed with hydrogen on Pt nanoparticles. This CO can form *in-situ* upon reduction of carbonates present on TiO_2 by photocatalytically formed hydrogen.[39] The red shift of $\nu(CO_{ads})$ in the presence of co-adsorbed hydrogen can be explained by dilution of adsorbed CO molecules on Pt nanoparticles[40] which weakens dipole coupling among them.[34]

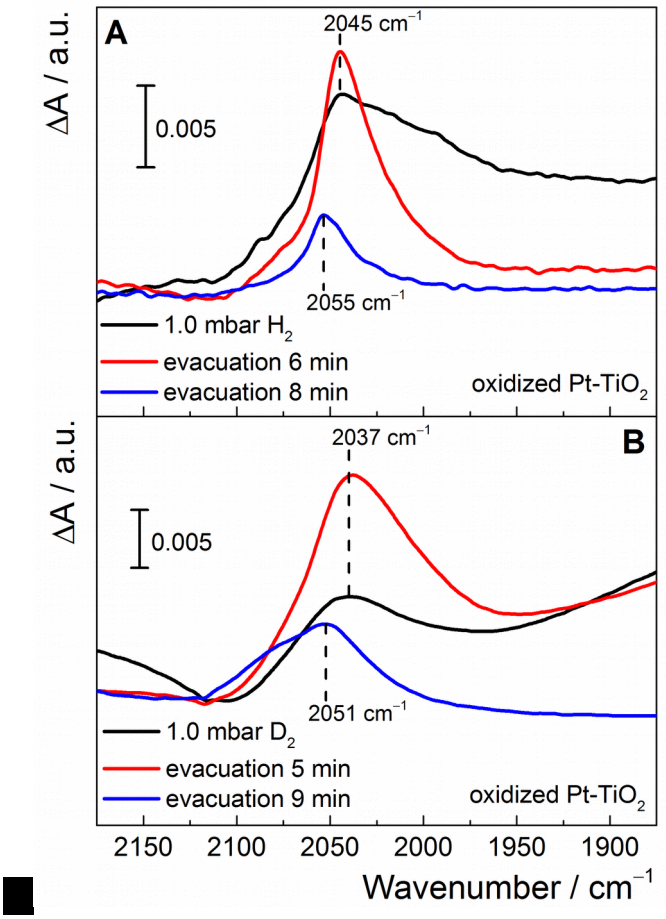

Figure 6. The carbonyl region of the difference DRIFT spectra of oxidized Pt-TiO_2 exposed to H_2 (A) and D-exchanged sample exposed to D_2 (B) at 293 K in the dark and upon evacuation of the gas.

CO adsorbed on Pt-CdS. The shift of the adsorbed CO bands induced by the charge transfer between a semiconductor and co-catalyst should be a generic property of metal-loaded semiconductor photocatalysts. Therefore, in addition to Pt-TiO_2, we investigated platinized CdS under 325 nm irradiation. In comparison to TiO_2, CdS has a narrower bandgap (2.42 eV) and

its conduction band is ca. 0.2 eV higher in energy.[42] Hence, one would expect a more prominent shift of the $\nu(CO_{ads})$ bands for Pt-CdS in comparison with Pt-TiO_2. When Pt-CdS was exposed to CO, an asymmetric band with a maximum at 2081 cm^{-1} emerged. This band can be ascribed to CO linearly adsorbed on metallic Pt.[33–35] Similarly to Pt-TiO_2, the position of $\nu(CO_{ads})$ band was not affected by UV irradiation (Figure S10, Supporting Information).

Discussion of the light-induced induced ν(CO) band shifts. Under 325 nm irradiation, neither Pt-TiO_2 nor Pt-CdS exhibited any prominent shifts of the adsorbed CO bands which can be unambiguously attributed to persistent charge transfer to the Pt particles. On the other hand, CO adsorbed on metal electrodes[42–44] or semiconductor-supported Pt particles[18,19] immersed in an aqueous electrolyte show shifts up to 50 cm^{-1}/V, when they are exposed to above-bandgap excitation or when an external electric bias is applied to the system. In order to understand this discrepancy one should consider that, in general, the effect of the applied electric field on the CO band is more prominent at the liquid/solid[18,19,42,43] interface than for the gas/solid[45–47] systems. In aqueous liquid/solid systems the electrical bias induces shifts of the CO band position in the order of 28-50 cm^{-1}/V, while the effect of the applied electrical field on the vibrational frequency of CO adsorbed at the gas/solid interface is in the order of 10^{-6} $cm^{-1}/(V/cm)$.[45–47] For both systems, the influence of the electric field on the vibrational frequencies of adsorbed CO can be described by the electrostatic Stark effect. However, different dielectric permittivities of vacuum and aqueous electrolytes[44] and the

presence of the electrochemical double layer at the liquid/solid interface leads to very prominent $\nu(CO_{ads})$ shifts observed under electrochemical conditions. On the other hand, the intensity of the electric field in vacuum is limited by the break-down voltage which allows for the band shifts in the order 10^{-2} cm^{-1}.[47] Interestingly, theoretical studies performed with CO adsorbed on small Cu and Au clusters predicted shifts of $\nu(CO_{ads})$ in order of tens of cm^{-1} upon addition or removal of one electron.[48,49]

By using a classical electrodynamics approach and approximating an average Pt nanoparticle with a solid sphere of radius R = 1 nm (Figure S9, Supporting Information), one can calculate the electrical field strength E at the surface of such a particle, when one electron ($Q = 1.6 \times 10^{-19}$ C) is added to or removed from the system:

$$E(x)=\frac{Q}{4\pi\varepsilon_0 R^2} \qquad (2)$$

where $\varepsilon_0 = 8.854 \times 10^{-12}$ F/m is vacuum permittivity. This rough approximation returns $E \approx 1.5$ MV/cm which would induce a shift of $\nu(CO_{ads})$ of about 15 cm^{-1}. However, we did not observe such prominent band shifts in our experiments. This can be explained by screening of the electrical charge by the d-band of the Pt metal[50] which was not taken into account by equation (2). A Pt nanoparticle with 1 nm radius (Figure S9, Supporting Information) contains about 250-300 atoms. Position and structure of the vibrational bands of adsorbed CO suggest that these particles are metallic. Therefore,

the electron gas can efficiently screen transferred electrical charge resulting in a substantially weaker effective electrical field on the surface of Pt nanoparticles than that estimated with the equation (2).[50] On the other hand, screening cannot explain why the bands of CO adsorbed on isolated Pt atoms were not prominently affected by above-bandgap irradiation (Figure 5). Such small metal clusters do not develop d-bands but can be described with molecular orbital theory. Therefore, trapping of a charge carrier by these species would prominently affect interaction of adsorbed CO molecules with Pt clusters and, consequently, the position of $\nu(CO_{ads})$. The absence of a prominent band shift of CO adsorbed on isolated Pt atoms can be due to high energy penalties of transferring one electron to an isolated metal atom which hinder such charge transfer.

Based on our experimental results we surmise that the 11 cm^{-1} red shift of the adsorbed CO band reported in literature[20] was due to light-induced physicochemical processes other than accumulation of photogenerated charge carrier on Pt nanoparticles. The most probable explanation of this shift is dilution of adsorbed CO by hydrogen produced upon photocatalytic reduction of adsorbed water.

Conclusion

The influence of UV irradiation on the vibrational bands of CO adsorbed at the gas-solid interface of platinized TiO_2 P25 and CdS was studied by DRIFT spectroscopy. No prominent shifts of the vibrational bands of CO adsorbed

on metallic Pt nanoparticles were observed under 325 nm irradiation in either systems. Exposure of Pt-TiO_2 to UV light caused a blue shift of *ca.* 0.5 cm^{-1} of the 2112–2114 cm^{-1} band corresponding to CO adsorbed on isolated, atomic Pt species. A similar rearrangement of this carbonyl band was observed upon heating of the material from 293 K to 383 K. Therefore, the effect of above-bandgap excitation on the adsorbed CO band positions cannot be unambiguously attributed to charge transfer between the oxide and Pt species. Prolonged UV irradiation of Pt-TiO_2, which has not been exposed to CO, resulted in formation of carbonyl bands at 2056 cm^{-1} and 2114 cm^{-1}. The 2056 cm^{-1} band was not observed upon adsorption/desorption of pure CO and was ascribed to CO co-adsorbed with hydrogen on metallic Pt nanoparticles. Partial reduction of adventitious carbonates and/or carboxylates by hydrogen produced upon photocatalytic water reduction was proposed as the pathway of CO formation under above-bandgap irradiation of Pt-TiO_2. Based on these experimental results we conclude that charge transfer between a semiconductor and a metal co-catalyst does not induce prominent band shifts of CO adsorbed at the gas/solid interface. This contrasts large shifts observed for liquid/solid interfaces and demonstrates that the dielectric properties of the medium are crucial for the formation of the electric field of the strength sufficient for prominent shifts of adsorbed CO bands.

Acknowledgements

The authors thank Elif Perşembe for the contribution to preliminary experiments for this study. This work is supported by NanoNextNL, a micro and nanotechnology consortium of the Government of The Netherlands and 130 partners: project NNNL.02B.08 CO2Fix-1.

References

(1) Hoffmann, M. R.; Martin, S. T.; Choi, W.; Bahnemann, D. W. *Chem. Rev.* **1995**, *95*, 69–96.

(2) Wang, H.; Zhang, L.; Chen, Z.; Hu, J.; Li, S.; Wang, Z.; Liu, J.; Wang, X. *Chem. Soc. Rev.* **2014**, *43*, 5234–5244.

(3) Moniz, S. J. A.; Shevlin, S. A.; Martin, D. J.; Guo, Z.-X.; Tang, J. *Energy Environ. Sci.* **2015**, *8*, 731–759.

(4) Tahir, M.; Amin, N. S. *Renew. Sustain. Energy Rev.* **2013**, *25*, 560–579.

(5) Osterloh, F. E. *Chem. Soc. Rev.* **2013**, *42*, 2294–2320.

(6) Acar, C.; Dincer, I.; Naterer, G. F. *Int. J. Energy Res.* **2016**, *40*, 1449–1473.

(7) Kudo, A.; Miseki, Y. *Chem. Soc. Rev.* **2009**, *38*, 253–278.

(8) Gao, M.-R.; Xu, Y.-F.; Jiang, J.; Yu, S.-H. *Chem. Soc. Rev.* **2013**, *42*, 2986–3017.

(9) Barroso, M.; Cowan, A. J.; Pendlebury, S. R.; Grätzel, M.; Klug, D. R.; Durrant, J. R. *J. Am. Chem. Soc.* **2011**, *133*, 14868–14871.

(10) Yang, J.; Wang, D.; Han, H.; Li, C. *Acc. Chem. Res.* **2013**, *46*, 1900–1909.

(11) Panayotov, D. A.; Burrows, S. P.; Morris, J. R. *J. Phys. Chem. C* **2012**, *116*, 4535–4544.

(12) Yamakata, A.; Ishibashi, T. A.; Onishi, H. *Chem. Phys. Lett.* **2001**, *333*, 271–277.

(13) Warren, D. S.; McQuillan, A. J. *J. Phys. Chem. B* **2004**, *108*, 19373–19379.

(14) Szczepankiewicz, S. H.; Colussi, A. J.; Hoffmann, M. R. *J. Phys. Chem. B* **2000**, *104*, 9842–9850.

(15) Zaera, F. *Chem. Rev.* **2012**, *112*, 2920–2986.

(16) Mojet, B. L.; Ebbesen, S. D.; Lefferts, L. *Chem. Soc. Rev.* **2010**, *39*, 4643.

(17) Blyholder, G. *J. Phys. Chem.* **1964**, *68*, 2772–2777.

(18) Lercher, J. A.; Gründling, C.; Eder-Mirth, G. *Catal. Today* **1996**, *27*, 353–376.

(19) Kappers, M. J.; Miller, J. T.; Koningsberger, D. C. *J. Phys. Chem.* **1996**, *100*, 3227–3236.

(20) Yoshida, M.; Yamakata, A.; Takanabe, K.; Kubota, J.; Osawa, M.; Domen, K. *J. Am. Chem. Soc.* **2009**, *131*, 13218–13219.

(21) Lu, X.; Bandara, A.; Katayama, M.; Yamakata, A.; Kubota, J.; Domen, K. *J. Phys. Chem. C* **2011**, *115*, 23902–23907.

(22) Shen, S.; Wang, X.; Ding, Q.; Jin, S.; Feng, Z.; Li, C. *Chinese J. Catal.* **2014**, *35*, 1900–1906.

(23) Litke, A.; Hofmann, J. P.; Weber, T.; Hensen, E. J. M. *Inorg. Chem.* **2015**, *54*, 9491–9498.

(24) Wang, Y.; Wang, Y.; Xu, R. *J. Phys. Chem. C* **2013**, *117*, 783–790.

(25) Yates, D. J. C. *J. Phys. Chem.* **1961**, *65*, 746–753.

(26) Primet, M.; Pichat, P.; Mathieu, M. V. *J. Phys. Chem.* **1971**, *75*, 1216–1220.

(27) In *Lange's Handbook Of Chemistry*; Dean, J. A., Ed.; McGraw-Hill: New York, 1999; p. 1466.

(28) Czekaj, I.; Wambach, J.; Kröcher, O. *Int. J. Mol. Sci.* **2009**, *10*, 4310–4329.

(29) Jackson, P.; Parfitt, G. D. *Trans. Faraday Soc.* **1971**, *67*, 2469.

(30) Griffiths, D. M.; Rochester, C. H. *J. Chem. Soc. Faraday Trans. 1 Phys. Chem. Condens. Phases* **1977**, *73*, 1510.

(31) Dobson, K. D.; McQuillan, A. J. *Spectrochim. Acta Part A Mol. Biomol. Spectrosc.* **1999**, *55*, 1395–1405.

(32) Ding, K.; Gulec, A.; Johnson, A. M.; Schweitzer, N. M.; Stucky, G. D.; Marks, L. D.; Stair, P. C. *Science (80-.).* **2015**, *350*, 189–192.

(33) Barshad, Y.; Zhou, X.; Gulari, E. *J. Catal.* **1985**, *94*, 128–141.

(34) Benvenutti, E. V.; Franken, L.; Moro, C. C.; Davanzo, C. U. *Langmuir* **1999**, *15*, 8140–8146.

(35) Gao, H.; Xu, W.; He, H.; Shi, X.; Zhang, X.; Tanaka, K. *Spectrochim. Acta Part A Mol. Biomol. Spectrosc.* **2008**, *71*, 1193–1198.

(36) Hammaker, R. M.; Francis, S. A.; Eischens, R. P. *Spectrochim. Acta* **1965**, *21*, 1295–1309.

(37) Bazzo, A.; Urakawa, A. *ChemSusChem* **2013**, *6*, 2095–2102.

(38) Dong, Y.; Hu, G.; Hu, X.; Xie, G.; Lu, J.; Luo, M. *J. Phys. Chem. C* **2013**, *117*, 12537–12543.

(39) Dixon, L. *J. Catal.* **1975**, *37*, 368–375.

(40) Primet, M.; Basset, J. M.; Mathieu, M. V.; Prettre, M. *J. Catal.* **1973**, *28*, 368–375.

(41) Craig, J. H. *Appl. Surf. Sci.* **1982**, *10*, 315–324.

(42) Xu, Y.; Schoonen, M. A. A. *Am. Mineral.* **2000**, *85*, 543–556.

(43) Kunimatsu, K. *J. Phys. Chem.* **1984**, *88*, 2195–2200.

(44) Beden, B.; Bewick, A.; Lamy, C. *J. Electroanal. Chem. Interfacial Electrochem.* **1983**, *148*, 147–160.

(45) Liao, M.; Zhang, Q. *J. Chem. Soc. Faraday Trans.* **1998**, *94*, 1301–1308.

(46) Lambert, D. K. *Phys. Rev. Lett.* **1983**, *50*, 2106–2109.

(47) Luo, J. S.; Tobin, R. G.; Lambert, D. K. *Chem. Phys. Lett.* **1993**, *204*, 445–450.

(48) Lambert, D. K. *J. Electron Spectros. Relat. Phenomena* **1983**, *30*, 59–64.

(49) Bagus, P. S.; Pacchioni, G. *J. Phys. Conf. Ser.* **2008**, *117*, 12003.

(50) Head-Gordon, M.; Tully, J. C. *Chem. Phys.* **1993**, *175*, 37–51.

(51) Ashcroft, N. W.; Mermin, N. D. In *Solid state physics*; Saunders College: Philadelphia, 1976; p. 826.